Study of Dynamic eICIC in a Realistic Urban Deployment

Pedersen, Klaus I.; Soret, Beatriz; Barcos, Sonia; Gerardino, Guillermo Andrés Pocovi; Wang, Hua

Published in:
IEEE 81st Vehicular Technology Conference (VTC Spring), 2015

DOI (link to publication from Publisher):
10.1109/vtcspring.2015.7146112

Publication date:
2015

Document Version
Accepted author manuscript, peer reviewed version

Study of Dynamic eICIC in a Realistic Urban Deployment

Klaus I. Pedersen*†, Beatriz Soret*, Sonia Barcos†, Guillermo Pocovi†, Hua Wang†

*Nokia Networks, †Aalborg University

***Abstract*—In this paper, we investigate the operation of eICIC in a realistic deployment based on site specific data from a dense urban European capital area. Rather than the classical semi-static and common network-wide configuration, the importance of having highly dynamic and distributed mechanisms that are able to adapt to local environment conditions is revealed. We propose a promising opportunistic cell association algorithm and a generalized method for fast muting adaptation. The performance results show that the traditional semi-static eICIC configuration leads to modest gains in realistic deployments, whereas the set of proposed fast dynamic eICIC algorithms leads to capacity gains on the order of 35-120% depending on the local environment characteristics. In the analysis of the performance results for the site specific use case, it is furthermore highlighted how those deviate from typical findings from 3GPP standardized HetNet scenarios.**

I. Introduction

To address downlink co-channel macro and pico interference problems, the Third Generation Partnership Project (3GPP) has standardized Enhanced Inter-Cell Interference Coordination (eICIC) for LTE networks. The fundamental principle of eICIC is to perform muting of certain subframes at the macro-layer to reduce interference towards the pico-users. One of the advantages of eICIC is that it offers increased flexibility for load balancing between macros and picos. Despite the relatively short time since the introduction of eICIC, the open literature includes an impressive number of related studies. To give a few examples, an overview of the eICIC scheme is available in [1] - [2]. In [3], the search for the optimal macrocell muting pattern is formulated as a utility maximization problem, and dynamic programming is used to solve it. In [4], the joint optimization of the muting configuration and assignment of users to macro and pico cells is studied as a network-wise utility maximization problem, subject to using the same muting pattern on all macrocells. As assumed for the majority of eICIC studies, the first implementations of eICIC will likely adjust the muting configuration and load balancing on time-scales of hours or days based on collected spatio-temporal network data [5]. For example, a centralized SON-based scheme for eICIC parameter optimization was presented in [6], along with demonstration of the benefits by using input from a radio network planning tool with data from a HetNet deployment in New York City. To the best of our knowledge, only two recent studies propose using *fast* eICIC muting adaptation in coherence with rapid traffic variations to further boost the performance [7] [8].

The main contribution of this article is a dynamic framework for autonomous operation of eICIC in a highly irregular network network deployment, based on data from a European capital area. The dynamic framework includes enhanced load balancing at each call setup and a general method for fast eICIC muting adaptation. The performance of the proposed fast dynamic algorithms is compared to semi-static SON-based schemes, where the eICIC-related parameters are set using a heuristic search approach to find the best parameters.

The rest of the paper is organized as follows: The algorithms for fast dynamic adjustment of muting patterns and load balancing are presented in Section II. Section III outlines the network model and considered performance metrics. Section IV presents the corresponding performance results, followed by concluding remarks in Section V.

II. Dynamic eICIC Strategies

A. User Association

In the majority of the published eICIC studies it is assumed that the serving cell index for the users is determined according to the following rule,

$$i^* = \arg\max_i \{P_{RSRP,i} + RE_i\} \,, \tag{1}$$

where $P_{RSRP,i}$ is the Reference Signal Received Power (RSRP) from cell i (in dBm) while RE_i is the Range Extension (RE) for cell i (in dB). Assuming $RE_i = 0$ dB for macrocells and $RE_i \geq 0$ dB for picocells, the setting of the RE parameter essentially determines the inter-layer load balancing, while neglecting potential benefits of intra-layer load balancing. A picocell with large value of RE is typically only able to schedule its users in the extended cell range area during the subframes where the macro is muted, and the pico-users therefore are exposed to significantly less interference. The muted subframes at the macro are referred to as Almost Blank Subframes (ABS) [2]. The value of the RE offset, which is signaled to the UEs using the Radio Resource Control (RRC) protocol, is adjusted on a relative slow time-scale in order to avoid excessive RRC signaling overhead at the air-interface.

In this study we consider a more elaborated dynamic user association algorithm at each connection setup (user arrival). Inspired by the opportunistic scheduling scheme by Knopp and Humblet [9], we propose an equivalent method for selecting the serving cell that offers the highest throughput to the user. We refer to this criterion as *opportunistic* cell selection, and it can be formally written as

$$i^* = \arg\max_{i \in \mathbf{F}} \{\hat{R}_i\} \,, \tag{2}$$

where i^* is the selected cell, $\hat{R}_i$ is the estimated throughput for the user in cell i and $\mathbf{F}$ is the set of feasible candidate cells that the UE can detect with a received power difference of maximum 15 dB as compared to the strongest received cell.

The estimated throughput for the user in cell i is simply approximated by using Shannon's capacity formula and assuming equal resource sharing between the users per cell, i.e.,

$$\hat{R}_i = \frac{1}{u_i + 1} W \log_2(1 + \hat{\Gamma}_i), \tag{3}$$

where W is the carrier bandwidth, and $\hat{\Gamma}_i$ is the conditional estimated wideband SINR for the UE if served by cell i. The value of $\hat{\Gamma}_i$ is obtained as

$$\hat{\Gamma}_i = \frac{P_i}{\sum_{n \neq i} P_n + N_0} \tag{4}$$

for all macrocells, where N_0 is the thermal noise power and P_i is the received power from cell i. If cell i is a picocell, the expression of $\hat{\Gamma}_i$ is modified to exclude the interference from the dominant macrocell in the denominator of (4), i.e. assuming ABS in the dominant macro. Note that the throughput estimation in (3) is rather simple and does not fully account for the dynamic system behavior: The estimate is optimistic for macrocells, since it does not capture the cost in terms of throughput when the macro mutes some subframes; and optimistic for the picocells, too, where the dominant macro is assumed to mute all the time.

B. Generalized Fast ABS

The distributed algorithm for fast autonomous ABS adjustment by each of the macrocells is based on the work originally presented in [7] [8]. The scheme relies on semi-static configuration of few subframes as normal transmission and ABS - also referred to as normal and mandatory ABS. During those semi-statically configured subframes, users are requested to perform time-domain restricted channel quality feedback measurements to reflect the quality depending on whether the macrocell is muting or not [8]. The remaining majority of subframes are called *optional* ABS. The optional ABS can be used as normal or ABS in accordance with the desired optimization criterion. The macrocells decide shortly before the beginning of the optional ABS if it shall be used for normal transmission or ABS. It is assumed that each macrocell makes such decisions autonomously without any explicit coordination with its neighboring macrocells. The macrocell bases its decisions on load measurements from the picocells within its geographical coverage area, as well as knowledge of its own carried load.

In the original algorithm [7], the load is monitored per cluster, where each cluster is composed of one macrocell and the associated picocells. However, in irregular deployments like the scenario considered in this study, it is likely that users associated to a picocell perceive different macro cells as the strongest interferer. To deal with it, we propose an enhancement to the algorithm such that the load report accounts only for the victim pico-users that have the particular macrocell requesting the load measure as their dominant interferer (i.e. the victim users of that aggressor cell). This is important since the macrocell uses the picocell load measures to quantify the benefit of using macrocell muting.

In further outlining the algorithm, we use the following notation: z and n denotes the number of subframes used as ABS and normal in the current ABS period, respectively. Further, $T_{ABS} \in N$ is the repetition period of the ABS pattern, $u_{\text{aggressor}}$ is the total number of users served by the aggressor macrocell, u_{victim} is the sum of users from the surrounding picocells that have the macrocell as their dominant aggressor, and $U = u_{\text{aggressor}} + u_{\text{victim}}$ is the total amount of affected users. Given these definitions, the dynamics of the algorithm is as follows: For each optional ABS, the algorithm ensures first of all that the ratio of macro users is served with an appropriate ratio of normal transmission subframes, i.e.

$$u_{\text{aggressor}} \;/\; U \;<\; n \;/\; T_{ABS}, \tag{5}$$

If (5) is fulfilled, then it is checked whether the ratio of ABS resources assigned so far is lower than the ratio of victim users, i.e.

$$u_{\text{victim}} \;/\; U \;>\; z \;/\; T_{ABS}. \tag{6}$$

If (6) is true, the current subframe is muted, and the victim users will have an opportunity to be scheduled in the next subframe. Otherwise, normal transmission is applied in the subframe. The algorithm ensures first of all the service of macro-users, since the coverage area of the macro eNB is much larger, and the macro cell-edge users do not have the option of being scheduled with reduced interference conditions. Each of the macrocells acquire the value of u_{victim} from load reports coming from the individual picocells; i.e. via inter-cell signaling.

III. Network Model and Performance Metrics

A. Site-specific network model

A three-dimensional (3D) topography map is used for the considered dense urban European capital area. The map contains 3D building data (i.e. building footprint and height) as well as information on streets, open squares, parks, etc. The area is dominated by multi-floor buildings. The building height varies, with an average height of 14 meters. Macro base stations are placed according to typical operator deployment in the considered area to provide complete blanket coverage [13]. The macro site antennas are deployed at different heights, taking the local environment characteristics into account in order to have good wide area coverage. The average macro antenna height is in the order of 30 meters, using a few degrees of antenna down-tilt. The considered network area includes hundreds of macro-sites with sectorized antennas. However, our performance analysis is based on data-collection only from a 1.2 km^2 segment of the area as pictured in Figure 1, consisting of a number of macro-sites as well as 30 pico cells with omni directional antennas. As indicated with solid lines in Figure 1, the total network area is further divided into 5 sub-regions, denoted Area 1 to 5. The areas have been selected to represent localized areas with different characteristics that are important for the performance of dynamic eICIC. To give a few examples, Area 4 has the highest density of picos per macro cell area, while Area 1 has picos deployed further away from the dominant macro.

The pico cells are deployed outdoors at 5 meters height in street canyons or at open squares according to the algorithm in [13] to improve the overall fifth-percentile (5%-ile) outage throughput of the network. Both macros and picos are transmitting at the same 10 MHz carrier at 2.6 GHz. The radio propagation characteristics are obtained by using

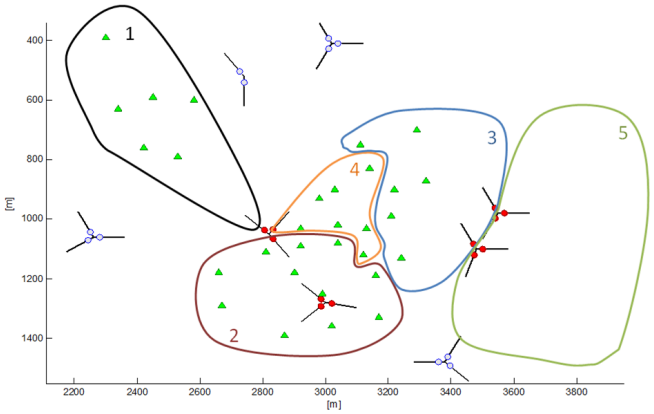

Fig. 1. Spatial location of macro and pico cells. The macro cells are marked with circles and a line pointing in the direction of the main lobe of the antenna (a.k.a. broadside). The triangular symbols mark pico cells with omni directional antennas.

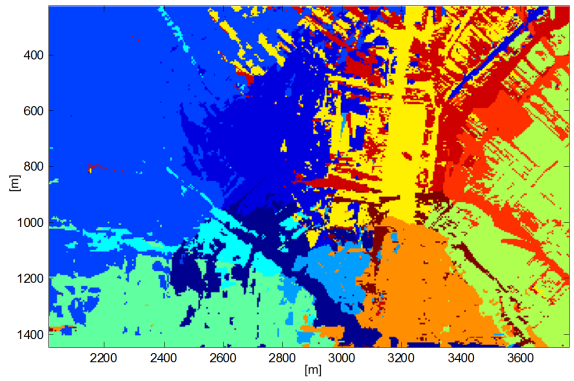

Fig. 2. Dominance area of the macro cells. Each colour represents different macro cells.

ray-tracing techniques based on the Dominant Path Model (DPM) [14] [15]. In coherence with observations from field measurements, outdoor-to-indoor propagation is modeled by including an additional 20 dB wall penetration loss as well as 0.6 dB per meter for the users placed inside the building [16]. Figure 2 shows the dominance area for the macrocells, where each colour represents different cells. Notice that the coverage area of each macrocell varies significantly, and deviates from the assumption of regular hexagonal cells as typically assumed for the generic 3GPP network models [11] [12].

B. Traffic modeling

A dynamic birth-death traffic model is assumed, where generation of new users is according to a standard Poisson point process with arrival rate λ. A fixed payload of B bits is assumed for each user. Once the payload has been successfully delivered to the user, the call is terminated and the user is removed. The average offered traffic load therefore equals $\overline{L} = \lambda \cdot B$. Whenever a new user is generated, the spatial location of the user in the horizontal plane is chosen randomly according to a discrete two-dimensional probability mass function. The probability mass function expresses the traffic density for each (horizontal) pixel of 10 x 10 meters for the considered area in line with [13]. For users that are placed at locations that coincide with multi-floor buildings, there is equal probability of placement per floor. The spatial traffic distribution is non-uniform with high variability of the traffic density per pixel. In fact, 80% of the users are indoor, although only 40% of the pixels represent areas with buildings. Furthermore, the 10% of the pixels with highest traffic density account for nearly 50% of the total offered traffic.

C. Performance metrics

The primary performance metric is the downlink end-user experienced data rate for each call. Based on a large number of samples of the users' data rates, the empirical cumulative distribution function (cdf) is built, enabling us to compute the 5%-ile outage and 50-percentile (50%-ile) experienced user throughput. The system capacity is defined as the maximum offered load that can be tolerated while still being able to serve at least 95% of the users with 2 Mbps. As the considered dense urban capital area is highly irregular, one has to be careful if samples from the entire network area are used for computing the defined performance metrics. The following two approaches are considered: (i) Global performance based on samples from users in the entire considered area, and (ii) Localized performance based on samples from users positioned in the defined Areas in Figure 1.

IV. Simulation Results and Analysis

A. Simulation Methodology and Assumptions

The performance of the proposed solution is evaluated with a system-level simulator following the LTE specifications, including detailed modeling of major RRM functionalities [17]. For each subframe of 1 ms, the experienced SINR for each scheduled user is calculated per sub-carrier, assuming an interference rejection combining (IRC) receiver [18]. Given the SINR per subcarrier, the effective exponential SINR model [19] for link-to-system-level mapping is applied to determine if the transmission was successfully decoded. Failed transmissions are retransmitted using hybrid ARQ with ideal Chase Combining (CC). The pico-users are configured to report separate channel quality measurement feedback when the macrocell is using normal transmission and ABS (and no measures taken during optional ABS) [2], [7], [8]. Closed loop 2x2 single user MIMO with pre-coding and rank adaptation is assumed for each link. Ideal cancellation of common reference signals (CRS) interference from ABS is further assumed for the pico-users [20]. Each cell schedules its users according to the Proportional Fair algorithm. The time-variant traffic model outlined in Section III-B is applied, assuming a payload size of B =4 Mbits for each call. In order to obtain statistically reliable results, simulations are run for a time-duration corresponding to at least 2800 completed calls. The default assumptions for the simulations are summarized in Table I.

B. Global Performance Statistics

We first present performance results based on the collection of statistics from the entire network, i.e. global performance. Figure 3 shows the 5%-ile and 50%-ile user throughput as a function of the average offered load in the whole network. The selected range of offered load corresponds to a system in

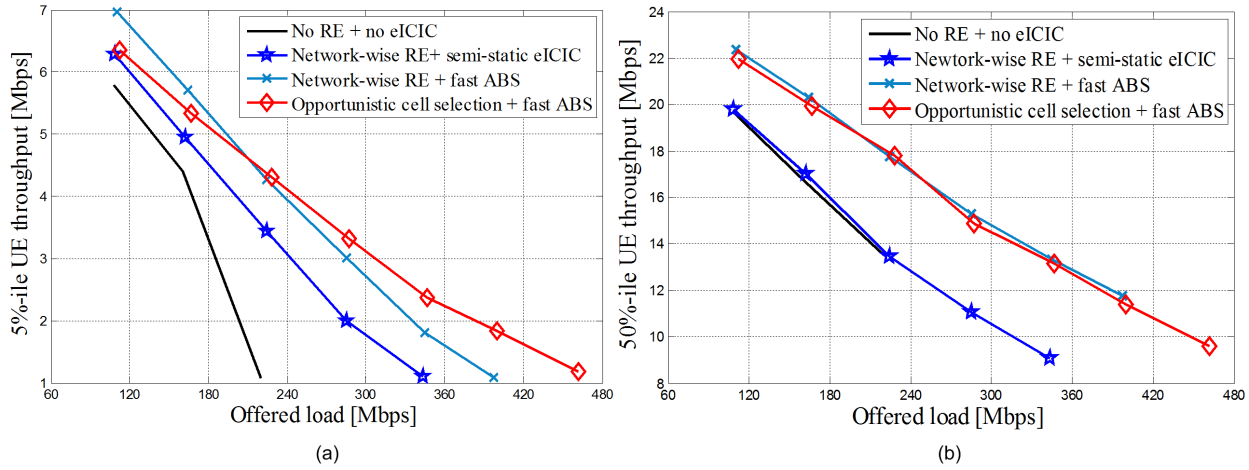

Fig. 3. Summary of attained network performance for all considered dynamic eICIC strategies. (a) 5%-ile user throughput (b) 50%-ile user throughput

TABLE I. SUMMARY OF DEFAULT SIMULATION ASSUMPTIONS

Transmit power	macro eNB: 46 dBm; pico eNB: 30 dBm
Bandwith	10 MHz at 2.6 GHz carrier frequency
Subframe duration	1 ms (11 data plus 3 control symbols)
Modulation and coding schemes	QPSK (1/5 to 3/4), 16-QAM (2/5 to 5/6), 64-QAM (3/5 to 9/10)
HARQ modeling	Ideal chase combining with maximum 4 transmissions, 10% block error rate target
Transmission mode	2x2 closed loop with rank adaptation
Antenna gain	Macro: 14 dBi; pico: 5 dBi; UE: 0 dBi
Antenna pattern	Macro: 3D pico and UE: omni directional
eNB packet scheduler	Proportional Fair (PF)
UE capabilities	Interference Rejection Combining; UEs with ideal CRS IC

equilibrium, where the carried traffic equals the offered load. Higher values of load would lead to congestion. The legend *Network-wise RE* refers to the case where user association is according to (1), assuming the same value of RE for all the picocells that maximizes the overall 5%-ile user throughput. Similarly, *semi-static eICIC* refers to the case where the same ABS muting pattern is used for all the macros. As expected, the user throughput decreases as the load in the network increases. When using network-wise RE and semi-static muting, the optimal value of the parameters varies with the offered load. At low offered load, a small value of RE is better, and there is little gain from applying macro muting. This is due to the fact that there is only marginal other-cell interference, and the gain in these low-loaded cases comes from the application of a small RE offset at the picocells. As the offered load increases, both macrocells and picocells start having higher probability of transmitting (and thus causing interference), and the system converges to use more ABS at the macrocells and higher RE at the picocells. In contrast to previous studies using 3GPP simulation scenarios [2], semi-static eICIC provides gains only for the 5%-ile user throughput, but not for the 50%-ile user throughput. Instead, the importance of fast ABS in highly irregular networks is clearly observed, leading to significant gains for both the 5%-ile and 50%-ile user throughput at the full range of considered offered traffic loads. Based on a closer inspection of the global user throughput statistics, it is found that the 5%-ile user throughput is primarily dominated by users positioned in Area 2 (see Figure 1). This is due to the highly irregular nature of the considered network; both in terms of site locations and the non-uniform spatial traffic distribution.

C. Local Performance Statistics

To gain further insight into the performance, we next analyze the local performance statistics collected for each of the defined network areas as illustrated in Figure 1. Figure 4 shows the gain in user throughput performance of the eICIC schemes for the different areas. These results are obtained by loading the network up to the maximum tolerable load for each area without using eICIC, followed by enabling eICIC to quantify the experienced increase in end-user throughput. Notice that Area 5 has no picocells and consequently there is no reason for applying eICIC (not shown in the Figure). In general, the eICIC performance gain is higher for the 5%-ile user throughput, although worth-while gains are also observed for the 50%-ile user throughput metric.

In Figure 5 the capacity gains for the different areas are plotted. Recall that capacity is defined as the maximum tolerable offered load while still being able to serve at least 95% of the users with a data rate of 2 Mbps. The capacity gain is given in terms of the relative improvement from having semi-static eICIC or dynamic eICIC as compared to no eICIC (and no RE). The results show substantial capacity gains of the dynamic eICIC for the considered areas, in the order of 35% to 120%. Here the fast ABS is responsible for most of the gains from using dynamic algorithms. The opportunistic dynamic cell selection techniques also provide benefits as it is the case of Area 2, thanks to their inter-cell load balancing capabilities. The highest gain from applying eICIC is observed for Area 2 and 4 as these regions are characterized by a relative higher number of picocells that are exposed to dominant macrocell interference. The highest capacity gain is achieved for Area 4.

The relatively large variability of the eICIC performance gain from one local area to another emphasizes the importance of basing the conclusions not only on the global performance statistics, but also on the analysis of the local performance statistics. Furthermore, as promising performance gains are observed for local network areas of different characteristics,

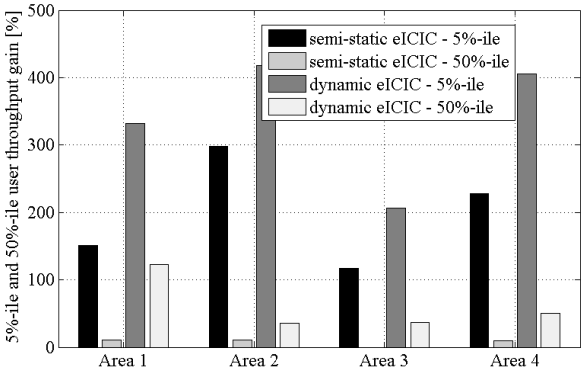

Fig. 4. 5%-ile and 50%-ile user throughput relative gains per area, as compared to baseline configuration with no eICIC.

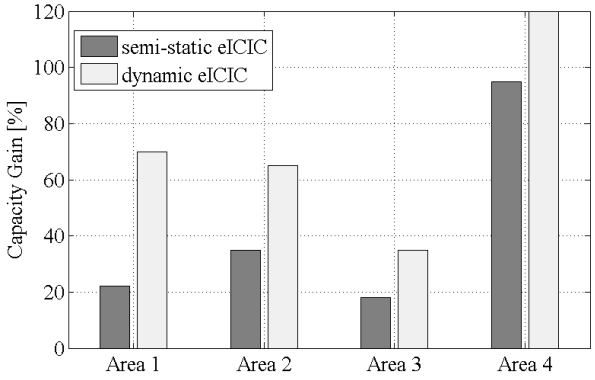

Fig. 5. Capacity gains of semi-static and dynamic eICIC per area, as compared to no eICIC. Capacity is defined here as the maximum tolerable offered load, while still being able to serve at least 95% of the users with a rate of 2 Mbps.

it suggests that the proposed scheme is generally applicable for other dense urban environments.

V. Conclusions

In this paper we have presented a fully dynamic framework with fast adjustment of the ABS muting at the macrocells and opportunistic cell association at each connection setup (user arrival). We have evaluated the performance of the proposed algorithms in a realistic network model based on data from segments of a irregular dense urban European capital area. As compared with semi-static SON-based schemes, where the eICIC-related parameters are set per network area using a heuristic search approach to find the best setting, the fast dynamic algorithms can track fast traffic fluctuations and autonomously adapt to the local network conditions. The joint use of opportunistic cell selection and generalized fast ABS provides a significant improvement in the studied KPIs (5%- and 50%-ile users throughput, and capacity gain). The findings shed additional light on the required network algorithms to harvest the full potential of eICIC in a practical setting.

References

[1] D. López-Pérez et al., "Enhanced Intercell Interference Coordination Challenges in Heterogeneous Networks," *IEEE Wireless Communications Magazine*, Pages 22-30, Vol. 18, Issue 3, June 2011.

[2] K.I. Pedersen, Y. Wang, S. Strzyz, and F. Frederiksen, "Enhanced Inter-Cell Interference Coordination in Co-Channel Multi-Layer LTE-Advanced Networks," *IEEE Wireless Communications Magazine*, June 2013.

[3] J. Pang, et.al., "Optimized Time-Domain Resource Partitioning for Enhanced Inter-Cell Interference Coordination in Heterogeneous Networks," *IEEE Wireless Communications and Networking Conference (WCNC)*, pp. 1613-1617, April 2012.

[4] A. Bedekar, and R. Agrawal, "Optimal Muting and Load Balancing for eICIC," *International Symposium and Workshops on Modeling and Optimization in Mobile, Ad Hoc and Wireless Networks (WiOpt)*, pp., 280-287, May 2013.

[5] S. Vasudevan, R. N. Pupala, and K. Sianesan, "Dynamic eICIC - A Proactive Strategy for Improving Spectral Efficiencies of Heterogeneous LTE Cellular Network by Leveraging User Mobility and Traffic Dynamics," *IEEE Transactions on Wireless Communications*, vol. 12, no. 10, pp. 4956-4969, October 2013.

[6] S. Dep, P. Monogioudis, J. Miernik, and J. P. Seymour, "Algorithms for Enhanced Inter-Cell Interference Coordination (eICIC) in LTE HetNets," *IEEE/ACM Transactions on Networking*, vol. 22, no. 1, February 2014.

[7] B. Soret, et.al., "Fast Muting Resource Allocation for LTE-A HetNets with Remote Radio Heads," *Proceedings IEEE Global Communications Conference (GLOBECOM)*, Dec. 2013.

[8] B. Soret, and K. I. Pedersen, "Centralized and Distributed Solutions for Fast Muting Adaptation in LTE-Advanced HetNets," *IEEE Transactions on Vehicular Technology*, 2014.

[9] R. Knopp, and P. A. Humblet, "Multiple-accessing over frequency-selective fading channel," *IEEE International Symposium on Personal, Indoor and Mobile Radio Communications PIMRC'95*, pp. 1326-1330, Sept. 1995.

[10] S. Hämäläinen, H. Sanneck, and C. Sartori, "LTE Self-Organizing Networks (SON): Network Management Automation for Operational Efficiency," *J. Wiley & Sons*, United Kingdom, 2012.

[11] 3GPP Technical Report 36.814, "Further Advancements for E-UTRA Physical Layer Aspects," version 9.0.0, March 2010.

[12] 3GPP Technical Report 36.872, "Small cell enhancements for E-UTRA and E-UTRAN Physical Layer Aspects," version 12.0.0, Sept. 2013.

[13] C. Coletti, et.al., "Heterogeneous Deployment to Meet Traffic Demand in a Realistic LTE Urban Scenario," IEEE Vehicular Technology Conference (VTC Fall), Sept. 2012.

[14] R. Wahl, et.al., "Dominant Path Prediction Model for Urban Scenarios", 14th IST Mobile and Wireless Communications Summit, Dresden (Germany), 2005.

[15] R. Wahl, G. Wolfle, "Combined urban and indoor network planning using the dominant path propagation model," First European Conference on Antennas and Propagation, EuCAP 2006, Nov. 2006.

[16] I. Rodriguez, et.al., "Path Loss Validation for Urban Micro Cell Scenarios at 3.5 GHz Compared to 1.9 GHz," IEEE Global Communications Conference (GLOBECOM), Dec. 2013.

[17] K. I. Pedersen, et.al., "An Overview of Downlink Radio Resource Management for UTRAN Long-Term Evolution," *IEEE Communications Magazine*, vol. 47, no. 7, pp. 86-93, July 2009.

[18] J. Winters, "Optimum combining in digital mobile radio with cochannel interference," *IEEE Journal on Selected Areas in Communications*, vol. 2, no. 4, pp. 528-539, July 1984.

[19] K. Brueninghaus, et.al., "Link performance models for system level simulations of broadband radio access systems," *IEEE Personal, Indoor and Mobile Radio Communications (PIMRC)*, pp. 2306-2311, Sept. 2005.

[20] B. Soret, Y. Wang, and K. I. Pedersen, "CRS Interference Cancellation in Heterogeneous Networks for LTE-Advanced Downlink", *IEEE International Conference on Communications ICC 2012 (International Workshop on Small Cell Wireless Networks)*, pp. 6797-6801, June 2012.